

PAPER

New Model of Flaming Phenomena in On-Line Social Networks Caused by Degenerated Oscillation Modes

Takahiro KUBO^{†a)}, Chisa TAKANO^{††}, and Masaki AIDA[†], *Members*

SUMMARY The explosive dynamics present in on-line social networks, typically represented by flaming phenomena, can have a serious impact on not only the sustainable operation of information networks but also on activities in the real world. In order to counter the flaming phenomenon, it is necessary to understand the mechanism underlying the generation of the flaming phenomena within an engineering framework. This paper discusses a new model of the generating mechanism of the flaming phenomena. Our previous study has shown that the cause of flaming phenomena can, by reference to an oscillation model on networks, be understood complex eigenvalues of the matrix formed to describe oscillating phenomena. In this paper, we show that the flaming phenomena can occur due to coupling between degenerated oscillation modes even if all the eigenvalues are real numbers. In addition, we investigate the generation process of flaming phenomena with respect to the initial phases of the degenerated oscillation modes.

key words: Laplacian matrix, directed graph, flaming, Jordan canonical form

1. Introduction

Recent developments in social networking services (social networks hereafter) have explosively activated information exchange among users. Active information exchange creates a situation where the activities of individual users of on-line social networks strongly influence each other. While such a situation has the positive effect of promoting the formation of active on-line communities of dynamic user, we recognize that more attention must be paid to the generation of negative effects. The user dynamics in on-line social networks can seriously impact on not only the sustainable operation of information networks, but also on activities in the real world. Typical examples are flash crowds on web servers and harmful rumors about disasters, respectively. Therefore, understanding the user dynamics present in on-line social networks is expected to yield important clues for resolving both issues. In particular, the flaming phenomena is a typical example of the negative influence caused by user dynamics; flaming refers the phenomena in which the strength of user dynamics, such as number of comments on SNS posts, becomes imbalanced due to the mutual influence among users. Since flaming phenomena arise frequently and are becoming

a significant social issue, it is important for the success of on-line social networks to understand of mechanism underlying the generation of the flaming phenomena and establish suitable countermeasure technologies [1].

This paper shows, from a theoretical point of view, that the flaming phenomena can occur due to coupling between degenerated oscillation modes in the oscillation model on networks even if all the eigenvalues are real numbers. This new model of the flaming phenomena, which is based on the coupling of oscillation modes, differs from the previous flaming phenomena model in that it allows the eigenvalues of the Laplacian matrix to be real numbers. To the best of our knowledge, this model is completely original.

This paper is organized as follows. In Sect. 2, we introduce some related work. Section 3 provides the preliminaries by briefly explaining the oscillation model on directed graphs and the fundamental equation that describes the oscillation model. In Sect. 4, we introduce and analyze the coupling effects caused by the degenerated oscillation modes. In Sect. 5, we investigate the relationship between the initial phase of the oscillation modes and occurrence of the flaming phenomena from the degenerated oscillation modes. Finally, we conclude this paper in Sect. 6.

2. Related Work

In various networks in the real world, the state of a node in networks is changed over time by the effect of other nodes through network links. Therefore, in order to know the node dynamics in networks, it is important to understand the effect of network links. Numerous studies dealing with network dynamics have been published [2]–[4]. In [2], malware propagation is studied by using a two layer epidemic model: the upper layer focuses on large scale networks, such as domains of the Internet, while the low layer model offers better accuracy than the single layer epidemic models used in malware modeling. In [3], the dynamics of an epidemic model are studied by using a susceptible-infected-susceptible epidemic model that incorporates with multistage infection (infection delay) and an infective medium (propagation vector) over complex networks, which typically exhibit nonlinear characteristics. In [4], consensus problems for networks with directed information flow are studied by analyzing three cases: 1) directed networks with fixed topology; 2) directed networks with switchable topology; and 3) undirected networks with communication time-delays and fixed topology. However, there has never been a model capable of describing

Manuscript received August 9, 2018.

Manuscript revised December 15, 2018.

Manuscript publicized January 24, 2019.

[†]The authors are with the Graduate School of Systems Design, Tokyo Metropolitan University, Hino-shi, 191-0065 Japan.

^{††}The author is with the Graduate School of Information Sciences, Hiroshima City University, Hiroshima-shi, 731-3194 Japan.

a) E-mail: kubo-takahiro@ed.tmu.ac.jp

DOI: 10.1587/transcom.2018EBT0002

the explosive user dynamics like the flaming phenomena in on-line social networks.

We have proposed an oscillation model on networks and clarified the divergence of the user state [1], [5], [6]. According to [7], [8], applying the oscillation model to networks can give a generalized concept of node centrality [9], [10], which indicates the strength of activity of network nodes. On this basis, we can define the flaming phenomena as a divergence in node centrality over an entire network [11]. In addition, we clarified that the flaming phenomena are caused by the Laplacian matrix representing the network structure having complex eigenvalues, and that flaming phenomena do not occur if the network structure has only eigenvalues of real numbers [1], [11]. On the other hand, there is true that some Laplacian matrices describing social networks cannot be diagonalized mathematically. That case yields dynamics greatly different from the case in which the Laplacian matrix can be diagonalized. In particular, the flaming phenomena can occur if the Laplacian matrix can not be diagonalized even if the eigenvalues of the Laplacian matrix are real numbers. However, those dynamics have not been examined so far.

The contribution of this study lies in dealing with a network structure in which the Laplacian matrix can not be diagonalized. In this study, we reveal a new mechanism that yields the flaming phenomena even if all the eigenvalues of the Laplacian matrix are real numbers.

3. Preliminaries

3.1 Oscillation Model on Directed Networks

On-line social networks must be modelled with directed graphs to describe the strengths of the influence between users, which are generally asymmetrical. Here, we introduce the oscillation model on on-line social networks [1].

The oscillation model on networks can simply describe the situation in which users influence each other. As this model, we consider the simplest and universal model, called the minimal model; it provides a simple expression of user states and universal interaction between users. To indicate the state of node i at time t , we assume that user state is written as the one-dimensional variable $x_i(t)$, where $i = 1, 2, \dots, n$ and n is the number of users. In addition, we define the state vector for all users as

$$\mathbf{x}(t) := {}^t(x_1(t), \dots, x_n(t)). \quad (1)$$

The interaction between users is described as follows. User i receives the force from neighboring node j such that the difference $|x_i(t) - x_j(t)|$ becomes small. The strength of the force is proportional to the difference $x_i(t) - x_j(t)$ as

$$-w_{ij}(x_i(t) - x_j(t)), \quad (2)$$

where $w_{ij} > 0$ is a constant. Since the interaction between users is asymmetrical, $w_{ij} \neq w_{ji}$ in general. Then, the equation of motion of the state vector of users is written as

$$\frac{d^2}{dt^2} \mathbf{x}(t) = -\mathcal{L} \mathbf{x}(t), \quad (3)$$

where \mathcal{L} is the Laplacian matrix [12] of the directed graph whose weight of directed link ($i \rightarrow j$) is given by w_{ij} . We can also consider the additional damping effect in the equation of motion. However, in order to focus on understanding the mechanism of generating flaming phenomena, this paper does not take the damping effect into consideration. We rewrite the equation of motion by expressing the Laplacian matrix in Jordan canonical form. Let the Jordan canonical form of \mathcal{L} be Λ . By using the square matrix $\mathbf{P} = [\mathbf{v}_1, \dots, \mathbf{v}_n]$ where \mathbf{v}_i ($i = 1, \dots, m, \dots, n$) is the generalized eigenvector of the Laplacian matrix \mathcal{L} , the Jordan canonical form of Λ is given by

$$\Lambda = \mathbf{P}^{-1} \mathcal{L} \mathbf{P}. \quad (4)$$

Then, we can write the equation of motion (3) as

$$\frac{d^2}{dt^2} \mathbf{y}(t) = -\Lambda \mathbf{y}(t), \quad (5)$$

where $\mathbf{y}(t) = \mathbf{P}^{-1} \mathbf{x}(t)$.

If Λ is diagonalizable, (5) is decomposed into the equation of motion of n independent harmonic oscillators as

$$\mathbf{y}(t) = \exp[\mp i \Lambda^{1/2} t] \mathbf{y}(0). \quad (6)$$

On the oscillation model for non-diagonalizable Λ , the equation of motion cannot be decomposed into independent harmonic oscillators due to the influence of the off-diagonal components of Λ . To explicitly understand the influence of the off-diagonal components, we use the fundamental equation [1]. First, we introduce an $n \times n$ matrix \mathbf{H} that satisfies

$$\mathbf{H}^2 = \Lambda. \quad (7)$$

Then, the fundamental equation of (5) is written as

$$\pm i \frac{d\boldsymbol{\phi}(t)}{dt} = \mathbf{H} \boldsymbol{\phi}(t). \quad (8)$$

The solution, $\boldsymbol{\phi}(t)$, of the fundamental equation (8) satisfies

$$\frac{d^2}{dt^2} \boldsymbol{\phi}(t) = \mp i \frac{d}{dt} \mathbf{H} \boldsymbol{\phi}(t) = -\mathbf{H}^2 \boldsymbol{\phi}(t),$$

the solution of (8) is also the solution of the original equation of motion (5). Although the method of determining \mathbf{H} from (7) is not unique, we can choose any \mathbf{H} that satisfies (7).

Note that the oscillation energy that is obtained from (6) gives the generalized notion of node centrality that includes the conventional degree centrality and the betweenness centrality [7], [8]. The node centrality expresses the strength of the activity of each node in the network. The oscillation model on directed graphs posits that no divergence in the oscillation energy occurs when the Laplacian matrix \mathcal{L} is diagonalizable and all the eigenvalues are real numbers. In other words, the diverge of the oscillation energy occurs only when at least one pair of eigenvalues are complex numbers

3.3 Simple Correspondence between Linear Operator Ω_J and the Network Structure

The linear operator Ω_J in fundamental equation (12) is not uniquely determined. In other words, we can select any Ω_J as long as H satisfies (7). When utilizing this degree of freedom to choose Ω_J , it is desirable to be able to make an explicit relationship between Ω_J and the structure of the original network.

First of all, we decompose non-diagonalizable matrix Ω_J^I into diagonal matrix $\Omega_J^{I(d)}$ and remainder matrix $\Omega_J^{I(a)}$ which has only off-diagonal components, as in

$$\Omega_J = \Omega_J^0 + \Omega_J^I = \Omega_J^0 + \Omega_J^{I(d)} + \Omega_J^{I(a)}. \quad (21)$$

The square of Ω_J is written as

$$\begin{aligned} \Omega_J^2 &= (\Omega_J^0)^2 + (\Omega_J^{I(d)})^2 + (\Omega_J^{I(a)})^2 \\ &\quad + \Omega_J^0 \Omega_J^{I(d)} + \Omega_J^{I(d)} \Omega_J^0 \\ &\quad + \Omega_J^0 \Omega_J^{I(a)} + \Omega_J^{I(a)} \Omega_J^0 \\ &\quad + \Omega_J^{I(d)} \Omega_J^{I(a)} + \Omega_J^{I(a)} \Omega_J^{I(d)}. \end{aligned} \quad (22)$$

If the following anti-commutation relations

$$\begin{aligned} \Omega_J^0 \Omega_J^{I(d)} &= -\Omega_J^{I(d)} \Omega_J^0 \\ \Omega_J^0 \Omega_J^{I(a)} &= -\Omega_J^{I(a)} \Omega_J^0 \\ \Omega_J^{I(d)} \Omega_J^{I(a)} &= -\Omega_J^{I(a)} \Omega_J^{I(d)} \end{aligned}$$

are established, all the cross terms in (22) can be canceled, and we can obtain the simple relation of

$$(\Omega_J^0)^2 + (\Omega_J^{I(d)})^2 + (\Omega_J^{I(a)})^2 = \Lambda_0 + \Lambda_I = \Lambda, \quad (23)$$

where Λ_0 is the diagonal matrix that satisfies $\Lambda_0 = (\Omega_J^0)^2$. That is, the network structure of the non-diagonalizable matrix is written as

$$\Lambda_I = (\Omega_J^{I(d)})^2 + (\Omega_J^{I(a)})^2. \quad (24)$$

The relation (24) can explicitly represent the correspondence between the Laplacian matrix and the non-diagonalizable part of Ω . If Ω is in Jordan canonical form, Λ simultaneously has Jordan canonical form.

The above anti-commutation relations are not true for the original matrices. However, by using the tensor product, we can introduce the anti-commutation relation to our model. We introduce the algebraic structure of the special unitary group $SU(2)$ by using Pauli matrices [13], [14]:

$$\sigma_1 = \begin{bmatrix} 0 & 1 \\ 1 & 0 \end{bmatrix}, \quad \sigma_2 = \begin{bmatrix} 0 & -i \\ i & 0 \end{bmatrix}, \quad \sigma_3 = \begin{bmatrix} 1 & 0 \\ 0 & -1 \end{bmatrix}.$$

For $i, j = 1, 2, 3$, the Pauli matrices satisfy the following relations:

$$\sigma_i^2 = E,$$

$$\sigma_i \sigma_j = -\sigma_j \sigma_i, \quad (i \neq j).$$

where E is the 2×2 identity matrix. By using the Pauli matrices, we convert the fundamental equation (12) as follows

$$\pm i \frac{d\hat{\psi}(t)}{dt} = \hat{\Omega}_J \hat{\psi}(t) = \left(\hat{\Omega}_J^0 + \hat{\Omega}_J^{I(d)} + \hat{\Omega}_J^{I(a)} \right) \hat{\psi}(t), \quad (25)$$

where

$$\begin{aligned} \hat{\Omega}_J^0 &:= \Omega_J^0 \otimes \sigma_3, \\ \hat{\Omega}_J^{I(d)} &:= \Omega_J^{I(d)} \otimes \sigma_1, \\ \hat{\Omega}_J^{I(a)} &:= \Omega_J^{I(a)} \otimes \sigma_2. \end{aligned} \quad (26)$$

In (26), \otimes represents the Kronecker product. $\hat{\Omega}_J$ is a $2m \times 2m$ square matrix and $\hat{\psi}(t)$ is a $2m$ -dimensional vector

$$\hat{\psi}(t) = {}^t(\psi_1^\uparrow(t), \psi_1^\downarrow(t), \psi_2^\uparrow(t), \psi_2^\downarrow(t), \dots, \psi_m^\uparrow(t), \psi_m^\downarrow(t)).$$

To simplify the calculation of (25), let us start from the unitary transformed version of the fundamental equation (20). The corresponding fundamental equation is written as

$$\pm i \frac{d\hat{\psi}(t)}{dt} = \left(\hat{\Omega}_J^0 + e^{\pm i \hat{\Omega}_J^0 t} \left(\hat{\Omega}_J^{I(d)} + \hat{\Omega}_J^{I(a)} \right) e^{\mp i \hat{\Omega}_J^0 t} \right) \hat{\psi}(t). \quad (27)$$

The solution is given by

$$\hat{\psi}(t) = \hat{\Psi}_0(t) \hat{\psi}_1(t), \quad (28)$$

where $\hat{\Psi}_0(t)$ is a $2m \times 2m$ diagonal matrix and $\hat{\psi}_1(t)$ is a $2m$ -dimensional vector that satisfy, respectively,

$$\pm i \frac{d\hat{\Psi}_0(t)}{dt} = \hat{\Omega}_J^0 \hat{\Psi}_0(t), \quad \pm i \frac{d\hat{\psi}_1(t)}{dt} = \hat{\Omega}_J^I \hat{\psi}_1(t). \quad (29)$$

Since $\hat{\Psi}_0(t) = \exp[\mp i \hat{\Omega}_J^0 t]$, the solution of (27) is expressed as

$$\hat{\psi}(t) = \exp(\mp i \hat{\Omega}_J^0 t) \hat{\psi}_1(t). \quad (30)$$

4. Coupling Effects Caused by Degenerated Oscillation Modes

4.1 Case Study of Three Degenerated Modes

Let us consider the simplest example of the degenerated oscillation modes. For example, a network structure that can exhibit triple degeneracy is the following. We provide below an example of the Laplacian matrix that encompasses real eigenvectors and degenerated oscillation modes.

$$\begin{bmatrix} 7 & -5 & -1 & 0 & -1 \\ -2 & 7 & -3 & -1 & -1 \\ -2 & -3 & 9 & -3 & -1 \\ -2 & -3 & -1 & 7 & -1 \\ -9/4 & -9/4 & -9/4 & -9/4 & 9 \end{bmatrix}. \quad (31)$$

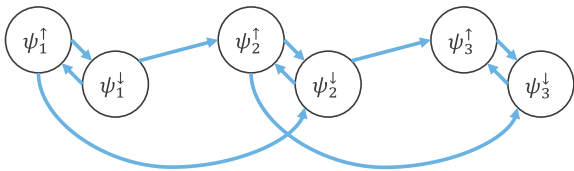


Fig. 1 Coupling of three pairs of oscillation modes.

This Laplacian matrix can be transformed into Jordan canonical form as follows

$$\begin{bmatrix} 0 & 0 & 0 & 0 & 0 \\ 0 & 9 & 0 & 0 & 0 \\ 0 & 0 & 10 & 1 & 0 \\ 0 & 0 & 0 & 10 & 1 \\ 0 & 0 & 0 & 0 & 10 \end{bmatrix}. \quad (32)$$

There is coupling among the three degenerated modes. For three degenerated modes selected from all modes of a directed graph, there are three pairs of oscillation modes (total six modes). Each oscillation mode interacts the other as shown in Fig. 1. The three pairs of oscillation modes are written as

$$\hat{\psi}(t) = {}^t(\psi_1^\uparrow(t), \psi_1^\downarrow(t), \psi_2^\uparrow(t), \psi_2^\downarrow(t), \psi_3^\uparrow(t), \psi_3^\downarrow(t)).$$

Then, the linear operators of $\hat{\Omega}_J$ are written as

$$\begin{aligned} \hat{\Omega}_J^0 &= \Omega_J^0 \otimes \sigma_3 = \begin{bmatrix} \omega & 0 & 0 \\ 0 & \omega & 0 \\ 0 & 0 & \omega \end{bmatrix} \otimes \sigma_3, \\ \hat{\Omega}_J^{I(d)} &= \Omega_J^{I(d)} \otimes \sigma_1 = \begin{bmatrix} d & 0 & 0 \\ 0 & d & 0 \\ 0 & 0 & d \end{bmatrix} \otimes \sigma_1, \\ \hat{\Omega}_J^{I(a)} &= \Omega_J^{I(a)} \otimes \sigma_2 = \begin{bmatrix} 0 & 1 & 0 \\ 0 & 0 & 1 \\ 0 & 0 & 0 \end{bmatrix} \otimes \sigma_2, \end{aligned} \quad (33)$$

where $\omega + d$ is the eigenfrequency of the degenerated oscillation modes.

We adopt the unitary transformed version of fundamental equation (27). From (33), we introduce the 6×6 matrix $\hat{\Omega}_J$ by using the Kronecker product of the Pauli matrices as

$$\begin{aligned} &\hat{\Omega}_J^0 + e^{+i\hat{\Omega}_J^0 t} \left(\hat{\Omega}_J^{I(d)} + \hat{\Omega}_J^{I(a)} \right) e^{-i\hat{\Omega}_J^0 t} \\ &= \Omega_J^0 \otimes \sigma_3 \\ &+ e^{+i\Omega_J^0 \otimes \sigma_3 t} \left(\Omega_J^{I(d)} \otimes \sigma_1 + \Omega_J^{I(a)} \otimes \sigma_2 \right) e^{-i\Omega_J^0 \otimes \sigma_3 t} \\ &= \begin{bmatrix} \omega & d e^{-i2\omega t} & 0 & -i e^{-i2\omega t} & 0 & 0 \\ d e^{+i2\omega t} & -\omega & i e^{+i2\omega t} & 0 & 0 & 0 \\ 0 & 0 & \omega & d e^{-i2\omega t} & 0 & -i e^{-i2\omega t} \\ 0 & 0 & d e^{+i2\omega t} & -\omega & i e^{+i2\omega t} & 0 \\ 0 & 0 & 0 & 0 & \omega & d e^{-i2\omega t} \\ 0 & 0 & 0 & 0 & d e^{+i2\omega t} & -\omega \end{bmatrix}. \end{aligned} \quad (34)$$

By using (25), (26) and (34), the fundamental equation is written as

$$\begin{aligned} &i \frac{d}{dt} \hat{\psi}(t) \\ &= \begin{bmatrix} \omega & d e^{-i2\omega t} & 0 & -i e^{-i2\omega t} & 0 & 0 \\ d e^{+i2\omega t} & -\omega & i e^{+i2\omega t} & 0 & 0 & 0 \\ 0 & 0 & \omega & d e^{-i2\omega t} & 0 & -i e^{-i2\omega t} \\ 0 & 0 & d e^{+i2\omega t} & -\omega & i e^{+i2\omega t} & 0 \\ 0 & 0 & 0 & 0 & \omega & d e^{-i2\omega t} \\ 0 & 0 & 0 & 0 & d e^{+i2\omega t} & -\omega \end{bmatrix} \hat{\psi}(t). \end{aligned} \quad (35)$$

The fundamental equation considers all oscillation modes (35). First, we introduce the phase differences $\delta_1^\uparrow(t)$, $\delta_1^\downarrow(t)$, $\delta_2^\uparrow(t)$, $\delta_2^\downarrow(t)$, $\delta_3^\uparrow(t)$, $\delta_3^\downarrow(t)$; they represent the phases of the oscillation modes of angular frequency $\mp\omega$. By using the phase difference, the solution of (35) is written as

$$\psi_1^\uparrow(t) = e^{-i\theta_1^\uparrow(t)} = e^{-i\omega t + i\delta_1^\uparrow(t)}, \quad (36)$$

$$\psi_1^\downarrow(t) = e^{+i\theta_1^\downarrow(t)} = e^{+i\omega t + i\delta_1^\downarrow(t)}. \quad (37)$$

$$\psi_2^\uparrow(t) = e^{-i\theta_2^\uparrow(t)} = e^{-i\omega t + i\delta_2^\uparrow(t)}, \quad (38)$$

$$\psi_2^\downarrow(t) = e^{+i\theta_2^\downarrow(t)} = e^{+i\omega t + i\delta_2^\downarrow(t)}. \quad (39)$$

$$\psi_3^\uparrow(t) = e^{-i\theta_3^\uparrow(t)} = e^{-i\omega t + i\delta_3^\uparrow(t)}, \quad (40)$$

$$\psi_3^\downarrow(t) = e^{+i\theta_3^\downarrow(t)} = e^{+i\omega t + i\delta_3^\downarrow(t)}. \quad (41)$$

By substituting (36) and (37) into fundamental equation (35), we have

$$\frac{d\delta_1^\uparrow(t)}{dt} = \omega + d e^{+i(\delta_1^\uparrow(t) - \delta_1^\downarrow(t))} - i e^{+i(\delta_2^\downarrow(t) - \delta_1^\uparrow(t))}, \quad (42)$$

$$\frac{d\delta_1^\downarrow(t)}{dt} = \omega - d e^{+i(\delta_1^\uparrow(t) - \delta_1^\downarrow(t))} - i e^{+i(\delta_2^\uparrow(t) - \delta_1^\downarrow(t))}. \quad (43)$$

Furthermore, by using the relationships of $\theta_1^\uparrow(t) = \omega t - \delta_1^\uparrow(t)$ and $\theta_1^\downarrow(t) = \omega t + \delta_1^\downarrow(t)$, we can write the temporal evolution equation of $\delta_1^\uparrow(t)$, $\delta_1^\downarrow(t)$ as

$$\frac{d\delta_1^\uparrow(t)}{dt} = -d e^{+i(\delta_1^\downarrow(t) - \delta_1^\uparrow(t))} + i e^{+i(\delta_2^\downarrow(t) - \delta_1^\uparrow(t))}, \quad (44)$$

$$\frac{d\delta_1^\downarrow(t)}{dt} = +d e^{+i(\delta_1^\uparrow(t) - \delta_1^\downarrow(t))} + i e^{+i(\delta_2^\uparrow(t) - \delta_1^\downarrow(t))}. \quad (45)$$

(44) and (45) represent the differential equations of the phase component of $\psi_1^\uparrow(t)$, $\psi_1^\downarrow(t)$. It is not always true that the phase differences are real numbers. Therefore, $\delta_1^\uparrow(t)$ and $\delta_1^\downarrow(t)$ are written as

$$\begin{aligned} \delta_1^\uparrow(t) &= \text{Re}[\delta_1^\uparrow(t)] + i \text{Im}[\delta_1^\uparrow(t)], \\ \delta_1^\downarrow(t) &= \text{Re}[\delta_1^\downarrow(t)] + i \text{Im}[\delta_1^\downarrow(t)]. \end{aligned} \quad (46)$$

By substituting (46) into equations (44) and (45), the temporal evolution equation of both the real and imaginary parts of $\delta_1^\uparrow(t)$ and $\delta_1^\downarrow(t)$ are written as

$$\begin{aligned} &\frac{d \text{Re}[\delta_1^\uparrow(t)]}{dt} = \\ &+ d e^{-\text{Im}[\delta_1^\downarrow(t)] + \text{Im}[\delta_1^\uparrow(t)]} \sin[\text{Re}[\delta_1^\downarrow(t)] - \text{Re}[\delta_1^\uparrow(t)] - \frac{\pi}{2}] \end{aligned}$$

$$+ e^{-\text{Im}[\delta_2^\downarrow(t)] + \text{Im}[\delta_1^\uparrow(t)]} \sin(\text{Re}[\delta_2^\downarrow(t)] - \text{Re}[\delta_1^\uparrow(t)] - \pi), \quad (47)$$

$$\begin{aligned} \frac{d \text{Re}[\delta_1^\downarrow(t)]}{dt} = & \\ & + d e^{+\text{Im}[\delta_1^\downarrow(t)] - \text{Im}[\delta_1^\uparrow(t)]} \sin(\text{Re}[\delta_1^\uparrow(t)] - \text{Re}[\delta_1^\downarrow(t)] + \frac{\pi}{2}) \\ & + e^{+\text{Im}[\delta_1^\downarrow(t)] - \text{Im}[\delta_2^\uparrow(t)]} \sin(\text{Re}[\delta_2^\uparrow(t)] - \text{Re}[\delta_1^\downarrow(t)] - \pi), \end{aligned} \quad (48)$$

$$\begin{aligned} \frac{d \text{Im}[\delta_1^\uparrow(t)]}{dt} = & \\ & + d e^{-\text{Im}[\delta_1^\downarrow(t)] + \text{Im}[\delta_1^\uparrow(t)]} \sin(\text{Re}[\delta_1^\downarrow(t)] - \text{Re}[\delta_1^\uparrow(t)] + \pi) \\ & + e^{-\text{Im}[\delta_2^\downarrow(t)] + \text{Im}[\delta_1^\uparrow(t)]} \sin(\text{Re}[\delta_2^\downarrow(t)] - \text{Re}[\delta_1^\uparrow(t)] + \frac{\pi}{2}), \end{aligned} \quad (49)$$

$$\begin{aligned} \frac{d \text{Im}[\delta_1^\downarrow(t)]}{dt} = & \\ & + d e^{+\text{Im}[\delta_1^\downarrow(t)] - \text{Im}[\delta_1^\uparrow(t)]} \sin(\text{Re}[\delta_1^\uparrow(t)] - \text{Re}[\delta_1^\downarrow(t)]) \\ & + e^{+\text{Im}[\delta_1^\downarrow(t)] - \text{Im}[\delta_2^\uparrow(t)]} \sin(\text{Re}[\delta_2^\uparrow(t)] - \text{Re}[\delta_1^\downarrow(t)] + \frac{\pi}{2}). \end{aligned} \quad (50)$$

The temporal evolution equations of the real parts (47), (48) are similar to the mathematical model used to describe synchronization, i.e., the so-called Kuramoto model [15]. The significant difference of (47), (48) from the Kuramoto model lies in the coefficients of the sine functions; the coefficients are not constant in our model. If the temporal change of the coefficients can be considered to be negligible, synchronization occurs also in our model. In this situation, the argument of the sine function becomes zero and phase synchronization occurs. If phase synchronization occurs in (47), $\text{Re}[\delta_1^\downarrow(t)]$ and $\text{Re}[\delta_1^\uparrow(t)]$ of the first term on the right-hand side synchronize with the phase difference of $\pi/2$. Figure 2 shows the relationship of the phase differences of $\text{Re}[\delta_1^\uparrow(t)]$, $\text{Re}[\delta_1^\downarrow(t)]$, $\text{Re}[\delta_2^\uparrow(t)]$ and $\text{Re}[\delta_2^\downarrow(t)]$ in the parentheses of the sine functions in (47) and (48) after synchronization.

Unlike the case of real parts, the temporal evolution equations of the imaginary parts (49) and (50) do not cause phase synchronization. However, if $\text{Re}[\delta_1^\downarrow(t)]$ and $\text{Re}[\delta_1^\uparrow(t)]$ cause phase synchronization, both arguments of the sine functions in the first and second terms of the right hand side of (49) and (50) become $3\pi/2$. If $d > 0$, the change

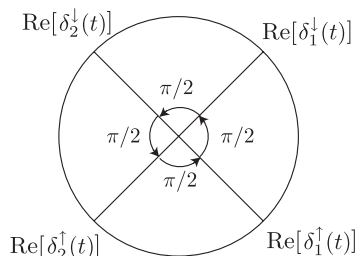


Fig. 2 Relationship of phase differences after synchronization.

rates of $\text{Im}[\delta_1^\uparrow(t)]$ and $\text{Im}[\delta_1^\downarrow(t)]$ are always negative because $\sin(3\pi/2) = -1$ on the right-hand side. By substituting the above results into (36) and (37), $\psi_1^\uparrow(t)$ and $\psi_1^\downarrow(t)$ are written as

$$\psi_1^\uparrow(t) = e^{-\text{Im}[\delta_1^\uparrow(t)]} e^{-i\omega t + i\text{Re}[\delta_1^\uparrow(t)]}, \quad (51)$$

$$\psi_1^\downarrow(t) = e^{-\text{Im}[\delta_1^\downarrow(t)]} e^{+i\omega t + i\text{Re}[\delta_1^\downarrow(t)]}. \quad (52)$$

If $\text{Re}[\delta_1^\uparrow(t)]$ and $\text{Re}[\delta_1^\downarrow(t)]$ are synchronized, (51) and (52) increase because $e^{-\text{Im}[\delta_1^\uparrow(t)]}$ and $e^{-\text{Im}[\delta_1^\downarrow(t)]}$ increase autonomously with time. The divergence of those terms increases triggering divergence of the oscillation energy, and this can be interpreted as a model that describes the flaming phenomena. The divergence of the oscillation energy is exponential as is the divergence of the flaming phenomena if the eigenvalues of the Laplacian matrix are complex numbers. However, there is a difference between the flaming phenomena caused by the degenerated oscillation modes and the flaming phenomena in the case that the eigenvalues of the Laplacian matrix are complex numbers. The emergence of the flaming phenomena caused by the degenerated oscillation modes can take time until divergence occurs because the oscillation modes go through a process of synchronization before divergence occurs. Using the model analyzed in this subsection, we confirmed that the flaming phenomena can occur due to coupling between degenerated oscillation modes even if all eigenvalues of \mathbf{H} are real numbers. This means that all eigenvalues of \mathcal{L} are also real numbers.

4.2 Numerical Experiments

In this subsection, we show the divergence of the solutions of the differential equations of the three pairs of degenerated oscillation modes to confirm the validity of the flaming model discussed in Sect. 4.1. In a similar way to Eqs. (47), (48), (49), and (50), the temporal evolution equation of both the real and imaginary parts of $\delta_2^\uparrow(t)$, $\delta_2^\downarrow(t)$, $\delta_3^\uparrow(t)$ and $\delta_3^\downarrow(t)$ are written as

$$\begin{aligned} \frac{d \text{Re}[\delta_2^\uparrow(t)]}{dt} = & \\ & + d e^{-\text{Im}[\delta_2^\downarrow(t)] + \text{Im}[\delta_2^\uparrow(t)]} \sin(\text{Re}[\delta_2^\downarrow(t)] - \text{Re}[\delta_2^\uparrow(t)] - \frac{\pi}{2}) \\ & + e^{-\text{Im}[\delta_3^\downarrow(t)] + \text{Im}[\delta_2^\uparrow(t)]} \sin(\text{Re}[\delta_3^\downarrow(t)] - \text{Re}[\delta_2^\uparrow(t)] - \pi), \end{aligned} \quad (53)$$

$$\begin{aligned} \frac{d \text{Re}[\delta_2^\downarrow(t)]}{dt} = & \\ & + d e^{+\text{Im}[\delta_2^\downarrow(t)] - \text{Im}[\delta_2^\uparrow(t)]} \sin(\text{Re}[\delta_2^\uparrow(t)] - \text{Re}[\delta_2^\downarrow(t)] + \frac{\pi}{2}) \\ & + e^{+\text{Im}[\delta_2^\downarrow(t)] - \text{Im}[\delta_3^\uparrow(t)]} \sin(\text{Re}[\delta_3^\uparrow(t)] - \text{Re}[\delta_2^\downarrow(t)] - \pi), \end{aligned} \quad (54)$$

$$\begin{aligned} \frac{d \text{Im}[\delta_2^\uparrow(t)]}{dt} = & \\ & + d e^{-\text{Im}[\delta_2^\downarrow(t)] + \text{Im}[\delta_2^\uparrow(t)]} \sin(\text{Re}[\delta_2^\downarrow(t)] - \text{Re}[\delta_2^\uparrow(t)] + \pi) \end{aligned}$$

Table 1 Parameters of initial phase.

Parameter	Value	Parameter	Value
d	1		
$\text{Re}[\delta_1^\uparrow(0)]$	0	$\text{Im}[\delta_1^\uparrow(0)]$	0
$\text{Re}[\delta_1^\downarrow(0)]$	0	$\text{Im}[\delta_1^\downarrow(0)]$	0
$\text{Re}[\delta_2^\uparrow(0)]$	0	$\text{Im}[\delta_2^\uparrow(0)]$	0
$\text{Re}[\delta_2^\downarrow(0)]$	0	$\text{Im}[\delta_2^\downarrow(0)]$	0
$\text{Re}[\delta_3^\uparrow(0)]$	0	$\text{Im}[\delta_3^\uparrow(0)]$	0
$\text{Re}[\delta_3^\downarrow(0)]$	0	$\text{Im}[\delta_3^\downarrow(0)]$	0

$$+ e^{-\text{Im}[\delta_3^\downarrow(t)] + \text{Im}[\delta_2^\uparrow(t)]} \sin(\text{Re}[\delta_3^\downarrow(t)] - \text{Re}[\delta_2^\uparrow(t)] + \frac{\pi}{2}), \quad (55)$$

$$\begin{aligned} \frac{d \text{Im}[\delta_2^\downarrow(t)]}{dt} = & \\ & + d e^{+\text{Im}[\delta_2^\downarrow(t)] - \text{Im}[\delta_2^\uparrow(t)]} \sin(\text{Re}[\delta_2^\uparrow(t)] - \text{Re}[\delta_2^\downarrow(t)]) \\ & + e^{+\text{Im}[\delta_2^\downarrow(t)] - \text{Im}[\delta_3^\uparrow(t)]} \sin(\text{Re}[\delta_3^\uparrow(t)] - \text{Re}[\delta_2^\downarrow(t)] + \frac{\pi}{2}), \end{aligned} \quad (56)$$

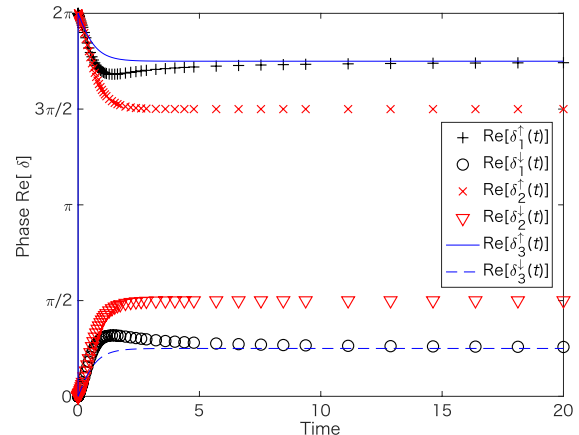
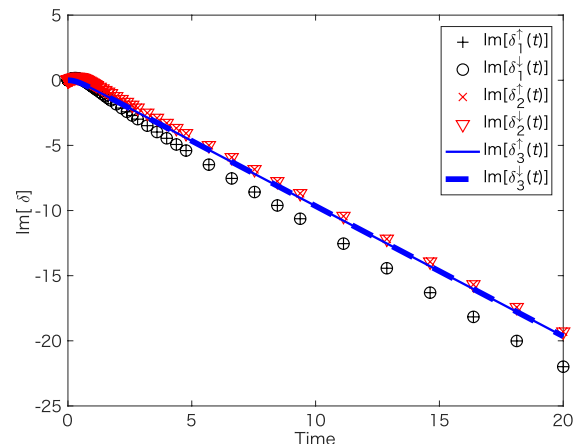
$$\begin{aligned} \frac{d \text{Re}[\delta_3^\uparrow(t)]}{dt} = & \\ & + d e^{-\text{Im}[\delta_3^\downarrow(t)] + \text{Im}[\delta_3^\uparrow(t)]} \sin(\text{Re}[\delta_3^\downarrow(t)] - \text{Re}[\delta_3^\uparrow(t)] - \frac{\pi}{2}), \end{aligned} \quad (57)$$

$$\begin{aligned} \frac{d \text{Re}[\delta_3^\downarrow(t)]}{dt} = & \\ & + d e^{+\text{Im}[\delta_3^\downarrow(t)] - \text{Im}[\delta_3^\uparrow(t)]} \sin(\text{Re}[\delta_3^\uparrow(t)] - \text{Re}[\delta_3^\downarrow(t)] + \frac{\pi}{2}), \end{aligned} \quad (58)$$

$$\begin{aligned} \frac{d \text{Im}[\delta_3^\uparrow(t)]}{dt} = & \\ & + d e^{-\text{Im}[\delta_3^\downarrow(t)] + \text{Im}[\delta_3^\uparrow(t)]} \sin(\text{Re}[\delta_3^\downarrow(t)] - \text{Re}[\delta_3^\uparrow(t)] + \pi), \end{aligned} \quad (59)$$

$$\begin{aligned} \frac{d \text{Im}[\delta_3^\downarrow(t)]}{dt} = & \\ & + d e^{+\text{Im}[\delta_3^\downarrow(t)] - \text{Im}[\delta_3^\uparrow(t)]} \sin(\text{Re}[\delta_3^\uparrow(t)] - \text{Re}[\delta_3^\downarrow(t)]). \end{aligned} \quad (60)$$

In the above differential equations, we set the value of d and the initial phase values at $t = 0$ as shown in Table 1. Figure 3 plots the phases of $\text{Re}[\delta_1^\uparrow(t)]$, $\text{Re}[\delta_1^\downarrow(t)]$, $\text{Re}[\delta_2^\uparrow(t)]$, $\text{Re}[\delta_2^\downarrow(t)]$, $\text{Re}[\delta_3^\uparrow(t)]$ and $\text{Re}[\delta_3^\downarrow(t)]$. The horizontal axis represents time t . With temporal evolution, it is shown that the phase difference of $\text{Re}[\delta_1^\uparrow(t)] - \text{Re}[\delta_1^\downarrow(t)]$ converges to $\pi/2$ as shown in Fig. 2. However, the phase differences of $\text{Re}[\delta_2^\downarrow(t)] - \text{Re}[\delta_1^\uparrow(t)]$ and $\text{Re}[\delta_2^\uparrow(t)] - \text{Re}[\delta_1^\downarrow(t)]$ do not converge to π and $3\pi/2$, respectively. The phase difference of $\text{Re}[\delta_3^\downarrow(t)] - \text{Re}[\delta_3^\uparrow(t)]$ converges to $\pi/2$. Although, Fig. 2 does not show the phase relation for $\text{Re}[\delta_3^\downarrow(t)]$, $\text{Re}[\delta_3^\uparrow(t)]$, we note that $\text{Re}[\delta_3^\downarrow(t)] - \text{Re}[\delta_3^\uparrow(t)]$ converges to $\pi/2$ from (57) and (58). In the next section, we will give a detailed analysis about the convergence of the phase differences of modes 1,

**Fig. 3** Numerical results of $\text{Re}[\delta_1^\uparrow(t)]$, $\text{Re}[\delta_1^\downarrow(t)]$, $\text{Re}[\delta_2^\uparrow(t)]$, $\text{Re}[\delta_2^\downarrow(t)]$, $\text{Re}[\delta_3^\uparrow(t)]$ and $\text{Re}[\delta_3^\downarrow(t)]$.**Fig. 4** Numerical results of $\text{Im}[\delta_1^\uparrow(t)]$, $\text{Im}[\delta_1^\downarrow(t)]$, $\text{Im}[\delta_2^\uparrow(t)]$, $\text{Im}[\delta_2^\downarrow(t)]$, $\text{Im}[\delta_3^\uparrow(t)]$ and $\text{Im}[\delta_3^\downarrow(t)]$.

2, and 3.

Figure 4 shows the numerical results of imaginary parts $\text{Im}[\delta_1^\uparrow(t)]$, $\text{Im}[\delta_1^\downarrow(t)]$, $\text{Im}[\delta_2^\uparrow(t)]$, $\text{Im}[\delta_2^\downarrow(t)]$, $\text{Im}[\delta_3^\uparrow(t)]$ and $\text{Im}[\delta_3^\downarrow(t)]$. The horizontal and vertical axis represent time and values of the imaginary parts, respectively. With temporal evolution, it is shown that values of the imaginary parts decrease in proportion to time. According to Sect. 4, $\text{Im}[\delta_1^\uparrow(t)]$, $\text{Im}[\delta_1^\downarrow(t)]$, $\text{Im}[\delta_2^\uparrow(t)]$, $\text{Im}[\delta_2^\downarrow(t)]$, $\text{Im}[\delta_3^\uparrow(t)]$ and $\text{Im}[\delta_3^\downarrow(t)]$ decrease after synchronization of $\text{Re}[\delta_1^\uparrow(t)]$, $\text{Re}[\delta_1^\downarrow(t)]$, $\text{Re}[\delta_2^\uparrow(t)]$, $\text{Re}[\delta_2^\downarrow(t)]$, $\text{Re}[\delta_3^\uparrow(t)]$ and $\text{Re}[\delta_3^\downarrow(t)]$. These results show that the decreases in the values of the imaginary parts are not bound, and indeed continue with time. By applying the numerical results of $\text{Im}[\delta_1^\uparrow(t)]$ and $\text{Im}[\delta_1^\downarrow(t)]$ to (51) and (52), $e^{-\text{Im}[\delta_1^\uparrow(t)]}$ and $e^{-\text{Im}[\delta_1^\downarrow(t)]}$ continue to increase exponentially with time. In the same way, it is shown that $e^{-\text{Im}[\delta_2^\uparrow(t)]}$, $e^{-\text{Im}[\delta_2^\downarrow(t)]}$, $e^{-\text{Im}[\delta_3^\uparrow(t)]}$ and $e^{-\text{Im}[\delta_3^\downarrow(t)]}$ continue to increase exponentially with time.

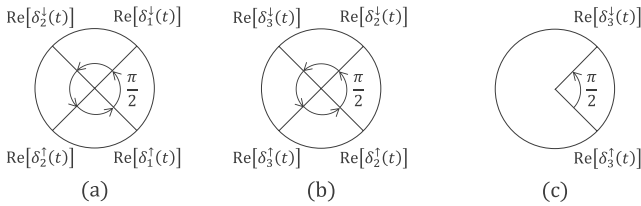


Fig. 5 Relationships of phase difference from each differential equation after synchronization.

5. Relationship between the Initial Phase and Divergence of the Degenerated Oscillation Modes

In this section, we show the relationship between the initial phase and divergence of the degenerated oscillation modes.

5.1 Theoretical Analysis

Figure 5 shows the relationship of expected mode synchronization plots from the temporal evolution equations of oscillation modes 1, 2, and 3. In Figs. 5(a), (b), and (c), a circle represents the unit circle in the complex plane. Those relations are obtained from the equations of phase differences of oscillation modes 1, 2, and 3, respectively. As the absolute position on the unit circle has no import, we focus on just the phase difference [16]. If the arguments of the sine functions become 0 from (47) and (48) due to Kuramoto-like synchronization, the relationship of Fig. 5(a) is obtained. The relationships in Fig. 5(b), and (c) are obtained in the same manner.

Although Fig. 5(a) is obtained from Eqs. (47) and (48) for $\text{Re}[\delta_1^\uparrow(t)]$ and $\text{Re}[\delta_1^\downarrow(t)]$, it is also associated with the phase differences for $\text{Re}[\delta_2^\uparrow(t)]$ and $\text{Re}[\delta_2^\downarrow(t)]$. In addition, (b) is obtained from the equations for $\text{Re}[\delta_2^\uparrow(t)]$ and $\text{Re}[\delta_2^\downarrow(t)]$, it is also associated with the phase differences for $\text{Re}[\delta_3^\uparrow(t)]$ and $\text{Re}[\delta_3^\downarrow(t)]$. Note that (a), (b), and (c) in Fig. 5 do not occur simultaneously due to the contradictory phase relationship. For example, the phase of $\text{Re}[\delta_2^\uparrow(t)]$ is advanced by $\pi/2$ from the phase of $\text{Re}[\delta_2^\downarrow(t)]$ in Fig. 5(a). However, the phase of $\text{Re}[\delta_2^\uparrow(t)]$ is delayed by $\pi/2$ from the phase of $\text{Re}[\delta_2^\downarrow(t)]$. Therefore, the phase relation of $\text{Re}[\delta_2^\uparrow(t)]$ and $\text{Re}[\delta_2^\downarrow(t)]$, which satisfies Fig. 5(a) and (b) simultaneously, can not exist. Similarly, the phase relation of $\text{Re}[\delta_3^\uparrow(t)]$ and $\text{Re}[\delta_3^\downarrow(t)]$ which satisfies Fig. 5(b) and (c) simultaneously can not exist.

In order to prevent the divergence of the oscillation mode, it is sufficient to prevent the temporal evolution equation from falling into Kuramoto-like synchronization. Given oscillation mode 1, based on the synchronized state in Fig. 5(a) which is obtained from Eqs. (47) and (48) for $\text{Re}[\delta_1^\uparrow(t)]$ and $\text{Re}[\delta_1^\downarrow(t)]$, we can set the initial phase as the reverse phase, which is considered to be most difficult to synchronize. However, if we provide the reverse phase of the

Table 2 Initial phase parameters.

Parameter	Value	Parameter	Value
d	1		
$\text{Re}[\delta_1^\uparrow(0)]$	$-\pi/4$	$\text{Im}[\delta_1^\uparrow(0)]$	0
$\text{Re}[\delta_1^\downarrow(0)]$	$-3\pi/4$	$\text{Im}[\delta_1^\downarrow(0)]$	0
$\text{Re}[\delta_2^\uparrow(0)]$	$-3\pi/4$	$\text{Im}[\delta_2^\uparrow(0)]$	0
$\text{Re}[\delta_2^\downarrow(0)]$	$-\pi/4$	$\text{Im}[\delta_2^\downarrow(0)]$	0
$\text{Re}[\delta_3^\uparrow(0)]$	$-\pi/4$	$\text{Im}[\delta_3^\uparrow(0)]$	0
$\text{Re}[\delta_3^\downarrow(0)]$	$-3\pi/4$	$\text{Im}[\delta_3^\downarrow(0)]$	0

synchronized state for oscillation mode 1, the phase for oscillation mode 2 is more likely to realize synchronization. On the right-hand side of the second term of Eq. (47), $\text{Re}[\delta_2^\downarrow(t)]$ synchronizes with $\text{Re}[\delta_1^\uparrow(t)]$ by π . If the phase of $\text{Re}[\delta_2^\downarrow(t)]$ is advanced from the synchronized state by π to avoid the synchronization in Fig. 5(a), oscillation mode 2 enters the synchronized state because $\text{Re}[\delta_2^\uparrow(t)]$ is delayed by $\pi/2$ relative to $\text{Re}[\delta_2^\downarrow(t)]$ as shown in Fig. 5(b). This result indicates that preventing the synchronization of all phase differences simultaneously is difficult for all combinations of the initial phases.

If the real parts of phase difference trigger Kuramoto-like synchronization, the values of the imaginary parts decrease in proportion to time, and the oscillation energy diverges. If any of the oscillation modes diverge, the oscillation energy diverges. As a result, it can be seen that divergence of the oscillation energy can be triggered by the degenerated oscillation modes without regard to the initial phase.

5.2 Numerical Evaluation of Behavior of Oscillation Modes

In this subsection, we evaluate the behavior of the oscillation modes created by differences in the initial phases. By numerical simulation, we evaluate the behavior of the solution of differential equations for the three oscillation modes.

In the first evaluation, we evaluate the behavior of the solution on the condition that the initial states of the phase differences are set to the reverse phases of the synchronized states. However, as discussed in Sect. 5.1, we can not provide the reverse phases of the synchronized states for all oscillation modes at the same time. Therefore, we set the relationship of the phase difference of mode 1 and 3 to the reverse phases of the synchronized state. On the other hand, the relationship of the phase difference of mode 2 is set to that of the synchronized state. Table 2 shows the initial phase parameters used in the numerical simulations.

Figure 6(a) plots the real parts of phase of the oscillation modes over time. Oscillation mode 1 ($\text{Re}[\delta_1^\uparrow(t)]$, $\text{Re}[\delta_1^\downarrow(t)]$) triggered phase synchronization. Oscillation mode 2 ($\text{Re}[\delta_2^\uparrow(t)]$, $\text{Re}[\delta_2^\downarrow(t)]$) did not trigger phase synchronization because the initial state already realized phase synchronization. Oscillation mode 3 ($\text{Re}[\delta_3^\uparrow(t)]$, $\text{Re}[\delta_3^\downarrow(t)]$) also did not trigger phase synchronization and maintained the initial state continuously.

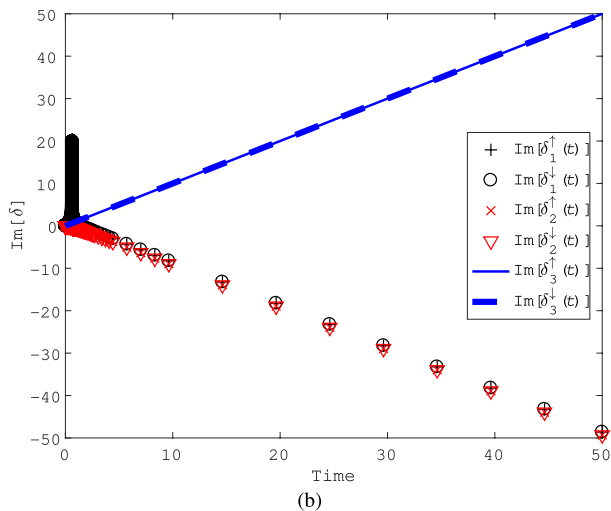
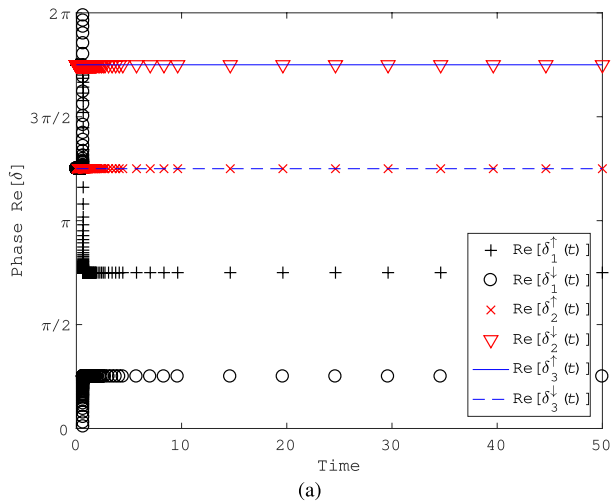


Fig. 6 Numerical results of real and imaginary parts of the phases of oscillation modes.

Figure 6(b) shows the imaginary parts of the phases of the oscillation modes. with attention to $\text{Im}[\delta_3^\downarrow(t)]$; it increases in proportion to time. This result indicates that the sine function of mode 3 did not become minus because $\text{Re}[\delta_3^\uparrow(t)]$ and $\text{Re}[\delta_3^\downarrow(t)]$ maintained the initial phase. However, the sine function of mode 2 held -1 because $\text{Re}[\delta_2^\uparrow(t)]$ and $\text{Re}[\delta_2^\downarrow(t)]$ maintained the initial phase. Therefore, with temporal evolution, it is shown that the imaginary parts of oscillation modes 1 and 2, which $\text{Re}[\delta_2^\uparrow(t)]$ and $\text{Re}[\delta_2^\downarrow(t)]$ contribute to, decrease in proportion to time. From this result, we can confirm divergence of the solutions over time even if the initial phases were the reverse of those in the synchronized state.

We evaluated the behavior of more diverged oscillation modes. We performed 1×10^4 times trials in which the real parts of the initial phases of oscillation modes 1, 2, and 3 at $t = 0$ were randomly set to a number between 0 and 2π . Figure 7 shows a histogram of the real parts

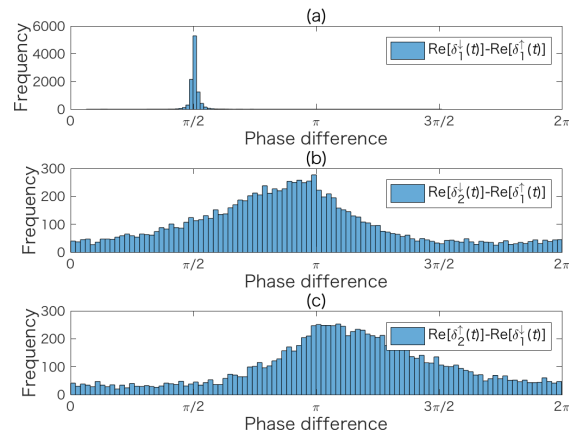


Fig. 7 Phase difference of mode 1 after sufficient time (a) $\text{Re}[\delta_1^\downarrow(t)] - \text{Re}[\delta_1^\uparrow(t)]$, (b) $\text{Re}[\delta_2^\downarrow(t)] - \text{Re}[\delta_1^\uparrow(t)]$, (c) $\text{Re}[\delta_2^\uparrow(t)] - \text{Re}[\delta_1^\downarrow(t)]$.

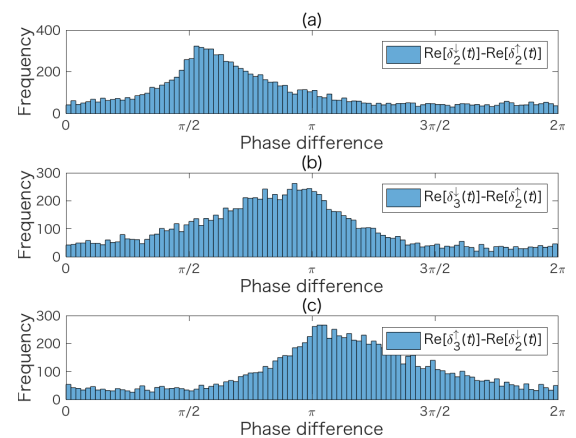


Fig. 8 Phase difference of mode 2 after sufficient time (a) $\text{Re}[\delta_2^\downarrow(t)] - \text{Re}[\delta_2^\uparrow(t)]$, (b) $\text{Re}[\delta_3^\uparrow(t)] - \text{Re}[\delta_2^\downarrow(t)]$, (c) $\text{Re}[\delta_3^\downarrow(t)] - \text{Re}[\delta_2^\uparrow(t)]$.

of the phase differences $\text{Re}[\delta_1^\downarrow(t)] - \text{Re}[\delta_1^\uparrow(t)]$, $\text{Re}[\delta_2^\downarrow(t)] - \text{Re}[\delta_1^\uparrow(t)]$, and $\text{Re}[\delta_2^\uparrow(t)] - \text{Re}[\delta_1^\downarrow(t)]$, that are related to mode 1, after sufficient time. In Fig. 7(a), the phase difference $\text{Re}[\delta_1^\downarrow(t)] - \text{Re}[\delta_1^\uparrow(t)]$ is mostly distributed around $\pi/2$, and exhibits Kuramoto-like synchronization.

On the other hand, Fig. 7(b) shows that the phase difference $\text{Re}[\delta_2^\downarrow(t)] - \text{Re}[\delta_1^\uparrow(t)]$ is widely distributed although some bias is observed for π . Figure 7(c) shows that the phase difference $\text{Re}[\delta_2^\uparrow(t)] - \text{Re}[\delta_1^\downarrow(t)]$ is widely distributed although some bias is observed for π , see Fig. 7(b). In these cases, signs of the sine function of the imaginary part are not specified. Therefore, it is unclear whether $\text{Im}[\delta_1^\uparrow(t)]$ or $\text{Im}[\delta_1^\downarrow(t)]$ decrease in proportion to time. Figure 8 shows a histogram of the real parts of the phase difference related to mode 2. Figure 8(b), (c) follow Fig. 7(b), (c). The difference is that Fig. 8(a) shows wider distributions than Fig. 7(a).

Although one of three oscillation modes does not contribute to the divergence of the oscillation energy, our interest is the possibility of oscillation energy divergence as a whole if the phase synchronization of other oscillation mode

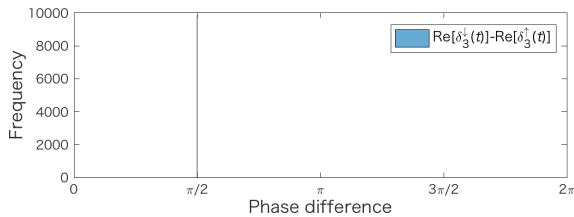


Fig. 9 Phase difference of mode 3 after sufficient time $\text{Re}[\delta_3^i(t)] - \text{Re}[\delta_3^T(t)]$.

contributes to the divergence of the oscillation energy. To examine the above possibility, we show the phase difference $\text{Re}[\delta_3^i(t)] - \text{Re}[\delta_3^T(t)]$, which is related to the sine function of the oscillation mode 3, in Fig. 9. From Fig. 9, the sine function turns negative because $\text{Re}[\delta_3^i(t)] - \text{Re}[\delta_3^T(t)] + \pi$, which is the parenthesis of the sine function in (59), synchronizes to $3\pi/2$. In a similar way, the sine function turned negative because $\text{Re}[\delta_3^T(t)] - \text{Re}[\delta_3^i(t)]$, which is the parenthesis of the sine function in (59), synchronizes to $3\pi/2$. As a result, the sine function in the right hand side of (59) and (60) is -1 . Then, the oscillation energy of mode 3 diverges because the imaginary part of the phase decreases. These results show that the degenerated oscillation modes can force divergence of the oscillation energy regardless of the initial phase.

6. Conclusion

This paper showed that the flaming phenomena can occur due to coupling between degenerated oscillation modes even if all eigenvalues are real numbers; this finding is quite different from previous studies on the flaming phenomenon which assume that the eigenvalues must be imaginary numbers. We adopted the Jordan canonical form of the linear operator corresponding to network structure to analyze the solution. This yields a simplified expression as the fundamental equation of the oscillation model on networks. If the linear operator cannot be diagonalized, we confirmed that the flaming phenomena can still occur due to oscillation mode divergence after the real parts of the phases of the degenerated oscillation modes synchroniz. Numerical simulations clearly showed the divergence of the solutions with time. We also investigated the relationship between the initial phases of the degenerated oscillation modes and oscillation energy divergence. Numerical simulations showed that divergence of the oscillation energy is independent of the initial phases of the degenerated oscillation modes.

References

- [1] M. Aida, C. Takano, and M. Murata, "Oscillation model for describing network dynamics caused by asymmetric node interaction," *IEICE Trans. Commun.*, vol.E101-B, no.1, pp.123–136, Jan. 2018.
- [2] S. Yu, G. Gu, A. Barnawi, S. Guo, and I. Stojenovic, "Malware propagation in large-scale networks," *IEEE Trans. Knowl. Data Eng.*, vol.27, no.1, pp.170–179, Jan. 2015.
- [3] A. Dadlani, M.S. Kumar, S. Murugan, and K. Kim, "System dynamics of a refined epidemic model for infection propagation over complex networks," *IEEE System Journal*, vol.10, no.4, pp.1316–1325, Nov. 2016.
- [4] R. Olfati-Saber and R.M. Murray, "Consensus problems in networks of agents with switching topology and time-delays," *IEEE Trans. Autom. Control*, vol.49, no.9, pp.1520–1533, Sept. 2014.
- [5] M. Aida, C. Takano, and M. Murata, "Oscillation model for network dynamics caused by asymmetric node interaction based on the symmetric scaled Laplacian matrix," The 12th International Conference on Foundations of Computer Science (FCS 2016), July 2016.
- [6] M. Aida, "Oscillation model for describing propagation of activities on network caused by asymmetric node interactions," Keynote Speech, IEICE Information and Communication Technology Forum 2016 (ICTF 2016), July 2016.
- [7] C. Takano and M. Aida, "Proposal of new index for describing node centralities based on oscillation dynamics on networks," *IEEE GLOBECOM 2016*, Dec. 2016.
- [8] C. Takano and M. Aida, "Revealing of the underlying mechanism of different node centralities based on oscillation dynamics on networks," *IEICE Trans. Commun.*, vol.E101-B, no.8, pp.1820–1832, Aug. 2018.
- [9] L.C. Freeman, "Centrality in social networks: Conceptual clarification," *Social Networks*, vol.1, no.3, pp.215–239, 1979.
- [10] L.C. Freeman, S.P. Borgatti, and D.R. White, "Centrality in valued graphs: A measure of betweenness based on network flow," *Social Networks*, vol.13, no.2, pp.141–154, 1991.
- [11] M. Aida, C. Takano, and M. Murata, "Dynamical model of flaming phenomena in on-line social networks," *IEEE/ACM International Conference on Social Networks Analysis and Mining (ASONAM 2017)*, pp.1164–1171, Sydney, Australia, 2017.
- [12] F.R.K. Chung, "Lectures on spectral graph theory," *CBMS Lecture Notes*, AMS Publications, Providence, 1995.
- [13] M. Aida, "Modelling and applications of oscillation dynamics on networks generated by asymmetric interaction between nodes," *IEICE Technical Report*, CCS2015-66, March 2016 (in Japanese).
- [14] T. Kubo, C. Takano, and M. Aida, "New model of flaming phenomena in on-line social networks caused by degenerated oscillation modes," *IEICE Technical Report*, NS2017-80, Sept. 2017 (in Japanese).
- [15] Y. Kuramoto, *Chemical Oscillations, Waves, and Turbulence*, Dover Books on Chemistry, 2003.
- [16] T. Kubo, C. Takano, and M. Aida, "Study on initial phase of model of flaming phenomena in on-line social networks caused by degenerated oscillation modes," *IEICE Technical Report*, NS2017-157, Jan. 2018 (in Japanese).



Takahiro Kubo received a B.S. degree in Physics from Tokyo Metropolitan University, Japan, in 2005, and a M.S. in Multidisciplinary Sciences from the University of Tokyo, Japan, in 2007. In 2007, he joined NTT Access Network Service Systems Laboratories, where he engaged in research on optical access systems using free space optics technologies. From 2013 to 2016, he worked with NTT DOCOMO, INC., where he worked on mobile radio access technologies. He is currently a graduate student, studying toward his Ph.D. degree at the Graduate School of Systems Design, Tokyo Metropolitan University. His current interest includes analysis of social network dynamics. He received the IEICE Young Researchers' Award in 2015. He is a member of the IEEE and IEICE.



Chisa Takano received a B.E. degree in Telecommunication Engineering from Osaka University, Japan, in 2000, and a Ph.D. in System Design Engineering from Tokyo Metropolitan University, Japan, in 2008. In 2000, she joined the Traffic Research Center, NTT Advanced Technology Corporation. Since April 2008, she has been an Associate Professor at the Graduate School of Information Sciences, Hiroshima City University. Her research interests are computer networks and distributed systems. She

received the IEICE Young Researchers' Award in 2003. She received the Information Network Research Awards from the IEICE in 2004, 2012, and 2015. She is a member of IEEE (U.S.A.).



Masaki Aida received his B.S. degree in Physics and M.S. degree in Atomic Physics from St. Paul's University, Tokyo, Japan, in 1987 and 1989, respectively, and his Ph.D. in Telecommunications Engineering from the University of Tokyo, Japan, in 1999. In April 1989, he joined NTT Laboratories. From April 2005 to March 2007, he was an Associate Professor at the Faculty of System Design, Tokyo Metropolitan University. He has been a Professor of the Graduate School of Systems Design, Tokyo Metropolitan

University since April 2007. His current interests include analysis of social network dynamics and distributed control of computer communication networks. He received the Best Tutorial Paper Award and the Best Paper Award of IEICE Communications Society in 2013 and 2016, respectively. He also received the IEICE 100-Year Memorial Paper Award in 2017. He is a member of the IEEE, ACM and the Operations Research Society of Japan.